

**FREQUENCY COMPARISON (H_MASER 40 0890) - (LNE-SYRTE-FO1)
From MJD 54084 to MJD 54099**

The primary frequency standard LNE-SYRTE-FO1 was compared to the hydrogen Maser (40 0890) of the laboratory during the 15th to 30th December 2006 period, from MJD 54084 to MJD 54099.

The mean frequency differences measured between the hydrogen Maser 40 0890 and fountain FO1 during this period is given in table 1.

| Period (MJD) | y(HMaser _{40 0890} - FO1) | u_B | u_A | $u_{link / maser}$ |
|---------------|------------------------------------|-------|-------|--------------------|
| 54084 – 54099 | -3790,0 | 4,0 | 4,8 | 3.0 |

Table 1: Results of the comparison in 1×10^{-16} .

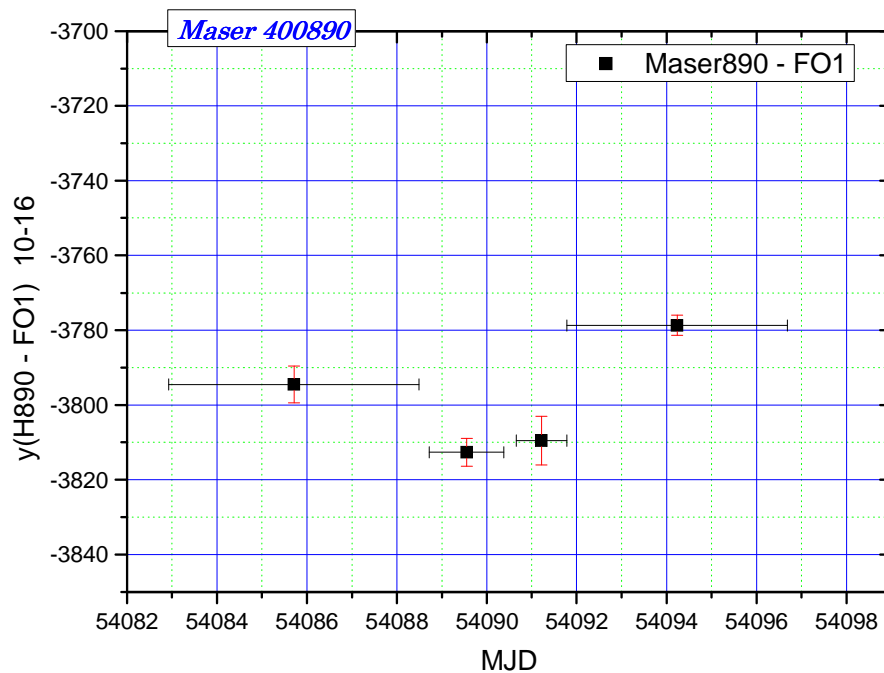


Figure 1: fractional frequency differences between Maser890 and FO1 measurements averaged over MJD 54084 to MJD 54099

Frequency average between the Maser 40 0890 and the SYRTE fountain FO1

Frequency measurements averaged over time interval of 12H of FO1 fountain were fitted over the period MJD 54084 to 54099 with a linear fit. Extrapolated frequency at the beginning and the ending of this period were estimated by this linear fit. A second iteration of the calculation of linear polynomial fitting also the extrapolated frequency was calculated. Figure 3 shows the frequency measurements averaged over time interval of 12H assorted by their statistical uncertainty and the frequency estimation at the limit of this period assorted by a larger statistical uncertainty issued from confidence bounds. The frequency average over the period MJD 54084-54099 is given by the frequency of the linear fit at the middle date of the period MJD 54084-54099, that correspond to the MJD 54091.5 and we obtain -3789.99×10^{-16} .

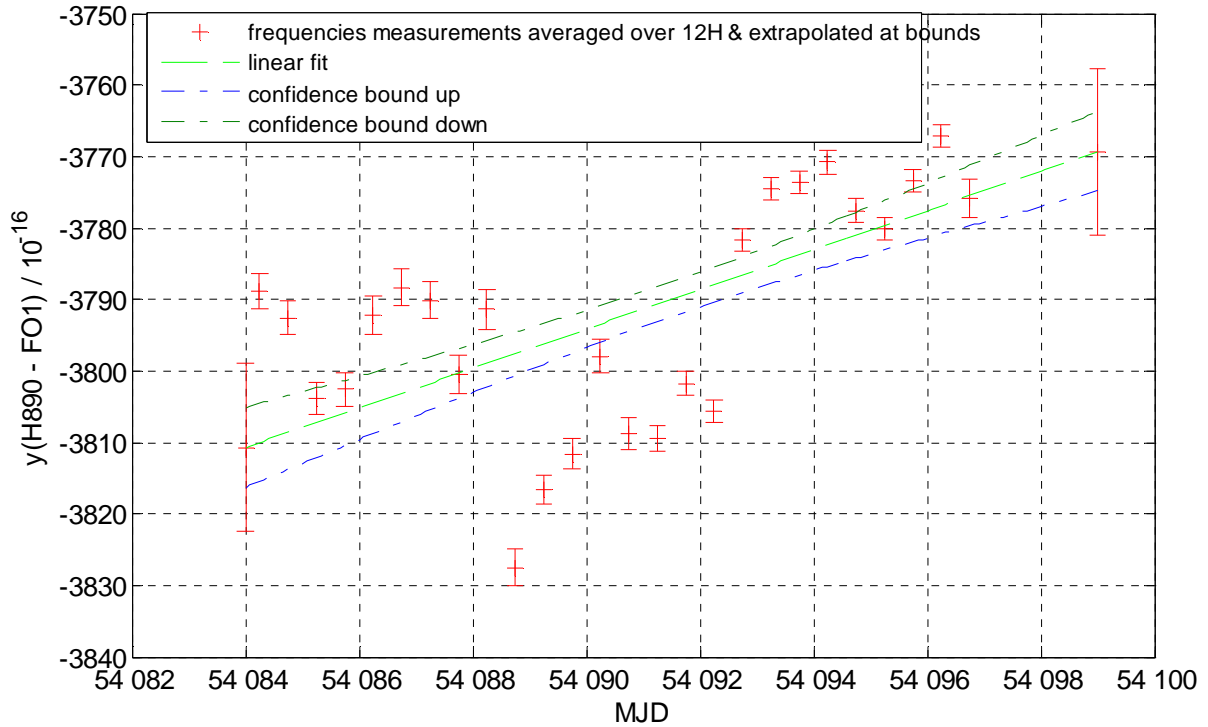


Figure 3: linear regression used to estimate the frequency average during period 54089-54095 of FO2 measurements

Statistical uncertainty on FO1 measurements

The uncertainty associated with this method of frequency average estimation is evaluated using the confidence bounds corresponding to +/- 1σ over the linear fit.

We found for the period MJD 54084 to MJD 54099

$$u_A = 4.78 \times 10^{-16}$$

Uncertainties budget of systematic effects in the FO1 fountain

Systematic effects taken into account are the quadratic Zeeman, the Black Body, the cold collision and cavity pulling corresponding to the systematic part, the microwave spectral purity and the microwave leakage, the Ramsey Rabi pulling, the recoil, the 1st and 2nd Doppler effects, and the background collisions. Each of these effects is affected by an uncertainty. The uncertainty of the red shift effect is also included in the systematic uncertainty budget [11]. Systematic uncertainty is estimated by the sum of quadratic systematic uncertainties.

Table 2 resumes the budget of systematic effects and their associated uncertainties. More details on systematic effects are developed in the next paragraphs.

| | Correction (10 ⁻¹⁶) | Uncertainty (10 ⁻¹⁶) |
|------------------------------------|---------------------------------|----------------------------------|
| Quadratic Zeeman effect | -1238.8 | 0.3 |
| Black body radiation | +165.7 | 0.6 |
| Cold collisions and cavity pulling | +262.9 | 1.3 |
| First order Doppler effect | | < 3.2 |
| Microwave spectral purity | | < 0.1 |
| Microwave leaks | | < 0.6 |
| Synchronous phase fluctuations | | < 0.6 |
| Background gas collisions | | < 0.3 |
| Microwave recoil | | < 1.4 |
| Ramsey & Rabi pulling | | < 0.1 |
| Second order Doppler effect | | < 0.1 |
| Total | | 3.9 |
| Red shift effect | 69,3 | 1.0 |
| Total with red shift | | 4.0 |

Table 2: budget of systematic effects and uncertainties for SYRTE-FO1 fountain

For the December 2006 period of measurement it gives

$$\sigma_B = 4.0 \cdot 10^{-16}$$

1 - Measurement of the 2nd order Zeeman frequency shift

Control of the magnetic field

The magnetic field instabilities due to thermoelectric currents are considerably reduced by operating the fountain with a homogeneous temperature. The magnetic field inside the drift zone is evaluated by measuring the frequency of the F=3, m_F=1 to F=4, m_F=1 transition. The central fringe of this transition is followed by slowly increasing the apogee height beginning in the cavity. Every 1000 s the 1-1 transition frequency is measured at full launch height. Over a 2 day period the measured field value drifts by less than 10⁻⁴ (relative). The Zeeman effect is corrected by averaging the magnetic field over this period.

The related uncertainty is based on the magnetic field drift. It is typically 3 x 10⁻¹⁷.

For central fringe averaged *MI* Hz, relative quadratic Zeeman shift is estimated by the mean of quadratic Zeeman shift

$$\frac{(\delta(\nu))_{Zeeman2}}{\nu_0} = 1.2388 \times 10^{-13} \quad , \quad \text{and an uncertainty } \sigma_{Zeeman2} = 2.5 \times 10^{-17}$$

2 - Measurement of the Blackbody Radiation shift

Control of the temperature

The entire set-up is at the ambient temperature. Apart from the stabilised laboratory temperature no active control exists. This reduces temperature gradients to the minimum. The temperature of the vacuum chamber made from OFHC copper is measured by 4-wire Pt100 resistors at the two extremities of the drift zone, i.e. 18 cm below the centre of the microwave cavity and 20 cm above the apogee. The temperature difference between the two points is 0.03 K. Their mean value differs from the laboratory temperature by 0.12 K, so that thermal radiation which might leak through the vacuum windows is identical to the inside radiation.

The calibration of the absolute temperature given by the two Pt100 resistors is known to 0.2 K. The temperatures are read every 30 s and used to correct the black body radiation shift in real time. The uncertainty of this correction contains the $2 \cdot 10^{-3}$ relative uncertainty of the coefficient to the T^4 term, the temperature gradient and the calibration uncertainty. It is of $6 \cdot 10^{-17}$ in relative frequency.

The average temperature is $T \sim 23,17^\circ\text{C}$. The correction is

$$\left(\frac{\delta(\nu)}{\nu_0} \right)_{\text{Blackbody}} = \frac{K_{BB} T^4 \left(1 + \frac{\varepsilon T^2}{T_0^2} \right)}{T_0^4}$$

with $K_{BB} = -1.573 \times 10^{-4} \pm 3 \times 10^{-7}$ [6], $\varepsilon := 0.014 \pm -0.0014$ [15], $T_0 := 300 \text{ K}$. The Blackbody

Radiation shift is assorted of uncertainty obtained with the squared of quadratic sum of $\delta(K_{BB})$

, $\delta(\varepsilon)$ and $\delta(T)$:

$$\frac{(\delta(\nu))_{\text{BlackBody}}}{\nu_0} = -165,7 \times 10^{-16} \pm 0,6 \times 10^{-16}$$

3 - Measurement of the collisional frequency shift and the cavity pulling

Control of the collisional shift and cavity pulling

Collisions between cold atoms in the cloud induce a shift of the transition frequency. In standard clock operation we alternate after 50 cycles between a configuration using 100% of the atoms and a configuration using 50%, while leaving the atom distribution within the cloud unchanged [4]. Thereby we can calculate the collision shift coefficient $K = (\text{freq}_{100\%} - \text{freq}_{50\%}) / (N_{100\%} - N_{50\%})$. The coefficient averages down with $\tau^{-1/2}$ and is known with a statistical resolution of $1.4 \cdot 10^{-2}$ after 4 days. Its mean value allows the correction of the collisional shift at each clock cycle as well as the cavity pulling. The frequency shift is typically 2×10^{-14} and hence the statistical uncertainty after a 15 day period is 1.4×10^{-16} . A systematic uncertainty stems from the fact that the ratio 50% is in practice not completely realised. The mean relative deviation is 2×10^{-3} . Furthermore, atomic states with $m_F \neq 0$ are populated to a fraction of 10^{-3} . The number of these atoms is not varied by our adiabatic passage method, hence the ratio 50% is not realised on this fraction of atoms. Their collisional effect on the clock transition is at most equivalent to the collisions of $m_F = 0$ atoms [6]. The number given in the table 2 is the quadratic sum of both statistical and systematic uncertainties. The relative frequency shift due to the effect of the collisions and "Cavity Pulling" of the atomic fountain FO1 taken in low density, between the MJD 54084 and 54099 with the statistical uncertainty $\sigma_{\text{Collision}(i)}$ were measured.

The mean of the collisional shift for the period of measurements in December is:

$$\frac{(\delta(\nu))_{Collision_Cavity_Pulling}}{\nu_0} = -2.6288 \times 10^{-14}$$

The overall systematic uncertainty is 8×10^{-17} and the statistical uncertainty for this 15 day period of this effect is 1.3×10^{-16} . This value is taking into account in the systematic uncertainty evaluation σ_B .

4 - Measurement of the residual 1st order Doppler effect

Control of the first order Doppler effect

In order to create a standing microwave inside the cavity in the most perfect way, the cavity is fed from two opposite sides. The coupling coefficients have been adapted to be equal before installing the cavity under vacuum. Under clock operation one can choose the supply path to be single left, single right or double with an attenuation of 70dB in the respective “off” path. The final adjustment is performed in observing the atomic response. Adjusting the supply power to induce a $\pi/4$ pulse on resonance, and therefore being sensitive to the microwave field amplitude, we find a 1dB difference (in power) between the left and the right path. To create a standing wave having the anti-node in the cavity centre, a variable phase shift is introduced into one path. The phase shift is adjusted by realising an almost $\pi/4$ pulse on resonance and maximising the atomic transition probability (Equilibrating the power and adjusting the phase shift may have to be repeated in an iterative way). In standard clock operation three configurations are alternated every 50 cycles corresponding to a supply only left, only right or symmetric. The overall power is automatically adjusted every 1700 s for each configuration by inducing a $\pi/2$ pulse on resonance. A symmetric supply should exclude any travelling wave within the microwave cavity. To verify this, we calculate the frequency differences $\text{freq_symm}-\text{freq_left}$ and $\text{freq_symm}-\text{freq_right}$. They are of order 5×10^{-16} with opposite sign. Their mean value fluctuates around 0. Averaging the mean value over the 15 day measurement period we find 5×10^{-18} with a statistical resolution of 1.2×10^{-16} . We take this value for the uncertainty due to the first order Doppler effect.

Another Doppler shift can occur due to the radial quadratic phase variation in the cavity. Taking an atom trajectory which passes through the cavity centre when rising and near the edges when falling this effect is maximum. We calculate the related shift to 3×10^{-16} . This is the largest uncertainty in the current clock evaluation. The quadratic sum of these shifts is given by:

$$\sigma_{FirstDoppler} = 3,2 \times 10^{-16}$$

5 - Effect of the Microwave Spectrum effect

Control of the microwave spectral purity

The interrogation signal carries sidebands to the 9.1926 GHz signal, where the nearest are 50 Hz from the carrier. Their power is 70dB below the carrier and the imbalance in power between the lower and upper sideband is smaller than 1dB. This leads to an upper limit of the induced frequency shift of 10^{-17} [2]. We find

$$\sigma_{Microwave_Spectrum_Purity} = 0,1 \times 10^{-16}$$

6 - Effect of the Microwave leakage

Control of microwave leaks

To minimise any effects of microwave leakage a high power micro-wave signal is generated at 8.91926 GHz and mixed with a low power radio frequency signal at 200 MHz as to generate only the necessary power at the transition frequency. Switching the RF part allows an attenuation of the output power by 45dB. In order to avoid any phase shift above 2 μ rad induced by the switching process, we use an interferometric switch [3]. Given our 1.1×10^{10} quality factor, such a phase shift would lead to a frequency uncertainty of less than 6×10^{-17} . The interferometric switch allows us to generate the interrogation signal only while the atoms are in the cavity. In fact we make the transition off/on and on/off when the centre of the atom cloud is in the centre of the respective cavity cut-off.

The effect of microwave leaks was evaluated in measuring the clock frequency in a configuration of continuous supply and a configuration of pulsed supply. A frequency difference of 1.5×10^{-15} was found, making the switching necessary. Therefore, in normal clock operation the interrogation signal is switched in the described way. Given the 45dB attenuation of the switch the effect of residual microwave is below 10^{-17} . We take the 6×10^{-17} uncertainty of the residual phase shift induced by the interferometric switch as the overall uncertainty.

$$\sigma_{\text{Microwave_Leakage}} = 0,6 \times 10^{-16}$$

7 – Synchronous phase fluctuations effect

Control of phase fluctuations synchronous with the clock cycle

Phase fluctuations synchronous with the clock cycle will not average away under multiples realisations. We have measure their presence by beating a fraction of the interrogation signal at 9.1926 GHz with a reference signal. The phase drift during the Ramsey times is smaller than 2 μ rad. This leads to a frequency uncertainty less than 6×10^{-17} .

$$\sigma_{\text{Phase_Fluctuations}} = 0,6 \times 10^{-16}$$

8 – Background collisions effect

Control of the back ground pressure

Due to the loading from the 2D MOT, the fountain vacuum chamber has the pressure as low as 3×10^{-8} pa. Hence the clock frequency shift due to collisions with the back ground gas is smaller than 3×10^{-17} [2].

9 – Microwave recoil effect

The shift due to the microwave photon recoil was investigated in [8]. It is smaller than 1.4×10^{-16} .

10 – Rabi and Ramsey effect and Majorana transitions effect

An imbalance between the residual populations and coherences of $m_F < 0$ and $m_F > 0$ states can lead to a shift of the clock frequency estimated to few 10^{-18} for a population imbalance of 10^{-3} that we observe in FO1 (see [9] and [10]).

11 – 2nd order Doppler shift

The 2nd order Doppler shift is less than 0.08×10^{-16} .

REFERENCES

- [1] - Li R., Gibble K. Phase variations in microwave cavities for atomic clocks, *Metrologia*, 2004, vol 41, pp 376-386.
- [2] - J. Vanier, C. Audouin, « The Quantum Physics of Atomic Frequency Standards », **Adam Hilger, Bristol & Philadelphia (1989)**.
- [3] - G. Santarelli *et al.*, Proceedings of the 2006 EFTF (2006).
- [4] - F. Pereira Do Santos, H. Marion, M. Abgrall, S. Zhang, Y. Sortais, S. Bize, I. Maksimovic, D. Calonico, J. Grünert, C. Mandache, C. Vian, P. Rosenbusch, P. Lemonde, G. Santarelli, Ph. Laurent and A. Clairon of LNE-SYRTE, C. Salomon of LKB, “Rb and Cs Laser Cooled Clocks: Testing the Stability of Fundamental Constants“. Proceedings IEEE 2003, EFTF Tampa May 2003, p 55-67.
- [5] - X. Baillard *et al* Opt. Comm. **266** 609 (2006)
- [6] - S. Bize et al , Advances in ¹³³Cs Fountains: Control of the Cold Collision Shift & Observation of Feshbach Resonances, Proceedings of ICAP 2004 Rio de Janeiro, Brazil, Atom Physics 19 p. 93-102.
- [7] - F. Pereira Do Santos, H. Marion, S. Bize, Y. Sortais, A. Clairon, and C. Solomon "Controlling the Cold Collision Shift in High Precision Atomic Interferometry" , **Phys. Rev. Lett. Vol. 89 number 23, 2002**.
- [8] - P. Wolf of LNE SYRTE, C.J. Bordé of LPL, “Recoil effects in microwave Ramsey spectroscopy”, arxiv: **quant-ph/0403194**.
- [9] - L. Cutler *et al*, “Frequency pulling by hyperfine σ - transitions in cesium atomic frequency standards, **J. Appl. Phys. Vol. 69, pp. 2780, 1991**.
- [10] - A. Bauch, R. Schröder “Frequency shift in Caesium Atomic Clock due to Majorana transitions”, *Annalen der Physik*, **vol. 2, pp. 421, 1993**.
- [11] - C. Vian, P. Rosenbusch, H. Marion, S. Bize, L. Cacciapuoti, S. Zhang, M. Abgrall, D. Chambon, I. Maksimovic, P. Laurent, G. Santarelli, A. Clairon of Obs. Paris, SYRTE, A. Luiten, M. Tobar, Univ. W. of Australia School of Physics, C. Salomon of LKB, “LNE-SYRTE Fountains: Recent Results”, **CPEM 2004, Proceedings IEEE Transactions on Instrumentation & Measurement, Vol. 54, NO. 2, April 2005**.
- [12] - F. Pereira Do Santos, H. Marion, M. Abgrall, S. Zhang, Y. Sortais, S. Bize, I. Maksimovic, D. Calonico, J. Grünert, C. Mandache, C. Vian, P. Rosenbusch, P. Lemonde, G. Santarelli, Ph. Laurent and A. Clairon of LNE-SYRTE, C. Salomon of LKB, “Rb and Cs Laser Cooled Clocks: Testing the Stability of Fundamental Constants“. **Proceedings IEEE 2003, EFTF Tampa May 2003, p 55-67**.
- [13] - R. Schröder, U. Hübner and D. Griebisch, “Design and Realization of the Microwave Cavity in PTB Caesium Atomic Clock CSF1” **IEEE Trans. Instrum. Meas., vol. 49, p.383, 2002**.
- [14] - H. Marion thèse de doctorat de l’Université de Paris 6 (Mars 2005)
- [15] - E. Simon, P. Laurent, and A. Clairon, Measurement of the Stark shift of the Cs hyperfine splitting in an atomic fountain, PRA vol.57 p.436 (1998)
- [16] - Wayne M. Itano and D. J. Wineland, Laser cooling of ions stored in harmonic and Penning traps, PRA vol.25, p.35 (1982)
- [17] - V G Pal'chikov *et al*, Black-body radiation effects and light shifts in atomic frequency standards *J. Opt. B: Quantum Semiclass. Opt.* **5** S131-S135 (2003)